

Received 6 July 2022, accepted 24 July 2022, date of publication 28 July 2022, date of current version 3 August 2022.

Digital Object Identifier 10.1109/ACCESS.2022.3194550

## RESEARCH ARTICLE

# Date Fruit Sorting Based on Deep Learning and Discriminant Correlation Analysis

OUSSAMA AIADI<sup>1,2</sup>, BELAL KHALDI<sup>1,2</sup>, MOHAMMED LAMINE KHERFI<sup>1,3</sup>,  
MOHAMED LAMINE MEKHALFI<sup>4</sup>, AND ABDULLAH ALHARBI<sup>5</sup>

<sup>1</sup>Department of Computer Science, University of Kasdi Merbah, Ouargla 30000, Algeria

<sup>2</sup>Artificial Intelligence and Information Technology Laboratory (LINATI), University of Kasdi Merbah, Ouargla 30000, Algeria

<sup>3</sup>LAMIA Laboratory, University of Quebec at Trois-Rivières, Trois-Rivières, QC G9A 5H7, Canada

<sup>4</sup>Digital Industry Center, Technologies of Vision, Fondazione Bruno Kessler, 38123 Trento, Italy

<sup>5</sup>Department of Computer Science, Community College, King Saud University, Riyadh 11437, Saudi Arabia

Corresponding author: Oussama Aiadi (aiadi.oussama@univ-ouargla.dz)

This work was supported by King Saud University, Riyadh, Saudi Arabia, under Grant RSP2022R444.

**ABSTRACT** Date fruit is among the major crops in the middle-east region, where millions of tons are harvested every year. Date is a healthy fruit, which involves sugars, minerals and vitamins. In addition, it helps preventing human body from several diseases such as cancer and heart diseases. Date sorting is a fundamental step in the date industry. However, manually conducting such an operation, by human labors, is expensive and time-consuming. In this paper, we propose a method for classifying the type of date fruit by incorporating supervised and unsupervised deep networks. Specifically, we use discriminant correlation analysis (DCA) algorithm to fuse features learned from convolution neural networks (VGG-F) and an unsupervised network called PCANet. DCA jointly performs feature fusion and dimensionality reduction with a low computational complexity. To carry out experiments, we introduce a new benchmark dataset of date fruit images from 20 date varieties. Our benchmark is, to the best of our knowledge, the largest one in terms of number of varieties. Note that the dataset is publicly available at <https://unsat.000webhostapp.com/dataset>. Experimental results demonstrate the utility of DCA as well as the complementarity of the fused features. It has also been shown the effectiveness of the proposed method compared to several relevant methods.

**INDEX TERMS** Classification, convolutional neural network, date fruit, sorting, deep learning, maturity.

## I. INTRODUCTION

With a total of more than 8 million tons produced in 2019 [1], date fruit is considered among the top crops in western Asia and the north Africa regions. Date fruit has different maturity levels (e.g., immature, semi-mature or mature) depending on the time at which it has been harvested. There exists numerous date varieties which differ from each other in terms of flavor, color and shape. In addition, date fruit provides a plenty of healthy benefits. In view of the sugars quantity it contains, date fruit is a vital source of energy. Besides, dates involve other elements such as minerals, vitamins and dietary fibers.

Date sorting is considered as an essential step in date industry. It consists in grading dates into different quality or

The associate editor coordinating the review of this manuscript and approving it for publication was Claudio Cusano<sup>1</sup>.

maturity levels. Another form of this process include classifying date fruit into different varieties. Manually performing such a job is boring, time-consuming, costly, and requires skilled employers. Therefore, there is a need for developing an automated computational system that can accomplish this procedure accurately. Typical examples on the use of date sorting process in our daily life include healthcare and commercial aspects. For instance, diabetics and obese persons need to determine the date cultivars they are authorized to eat and which maintain their health. In addition, a self-checkout system for recognizing different date cultivars in commercial centers is highly recommended [2].

In the two previous decades, several literature studies have addressed the problem of date sorting. Generally speaking, based on the aim they are targeting, these studies can broadly be categorized into three categories. The first category includes works aiming at detecting the quality of date

fruit [3], [4], whereas, in the second category, works are concerned with grading dates into different maturity levels [5], [6]. Regarding the third category, works contained therein are interested with classifying the variety to which a specific date sample, belongs [7], [8]. Due to its ability to learn reliable representations from images, deep learning has widely been applied to classify fruits instead the conventional approaches [9]. Deep approaches, especially convolutional neural networks (CNN), have been employed by several works for date sorting. While most existing works have opted for supervised deep-based schemes (e.g., CNN), a very little attention has been paid to the use of unsupervised deep networks for date fruit classification.

In this paper, we put forward a new method for date varieties classification based on deep learning techniques. In particular, we evaluate both supervised and unsupervised deep networks to this end. As a supervised network, we opt for the pre-trained VGG-F, as its depth is sufficient to extract robust local and global features from date fruit images. In addition, the more layers and parameters we have in the network, the more time it takes to extract features. Thus, considering a network with a small depth will reduce the processing time. As for the unsupervised network, we employ the PCANet, which has shown a good performance in many computer vision tasks in spite of its simplicity. To reinforce individual decisions produced by each type of networks, we opt for fusing both of the networks using discriminant correlation analysis (DCA) algorithm. DCA jointly performs feature-level fusion and dimensionality reduction with a low computational complexity by analyzing correlations among input features.

To evaluate the proposed method, we introduce a new dataset of date fruit, which includes images from twenty (20) varieties. Our dataset is the largest available dataset in terms of the number of varieties. Experimental results proved the complementarity of supervised and unsupervised networks, and demonstrated the effectiveness of the proposed method, which has outperformed several relevant methods. We summarize the contributions of the current paper as follows

- Demonstrating that date fruit sorting task can be accomplished using unsupervised deep networks PCANet) which has a lower computational cost than existing deep networks.
- Demonstrating that a supervised deep network with a small depth (i.e., VGG-F) is enough to perform the task of date fruit sorting.
- This study reveals also the complementarity of supervised and supervised networks which are fused using the DCA algorithm. This algorithm jointly performs fusion and dimensionality reduction with a low computational cost.
- Unlike the previous studies in most of which few number of date fruit varieties was considered, this study introduces a new dataset of date fruit that is made up of

twenty (20) date varieties. This dataset can be considered as the largest dataset in terms of the number of varieties.

- We carry out extensive experiments to measure the performance of the proposed method. Our method has significantly surpassed several deep and handcrafted methods from the state of the art.

The rest of this paper is organized as follows. In Section 2, we review the studies concerned with date fruit classification. Section 3 is dedicated to present the dataset we collected. In Section 4, we present the proposed method. Section 5 reports the findings of this study. A final section is Section 6, which is devoted to draw some conclusions and perspectives.

## II. RELATED WORK

Existing works on automatic date fruit processing can be classified into three main classes namely type classification, quality determination and maturity degree detection.

Early attempts for type classification back to the work of [10] in which physical attributes of seven date cultivars which are Berhi, Khlass, Nubot Saif, Saqei, Sefri, Serri, and Sukkari, were taken and fed to a neural network classifier. In [11], five date varieties were classified based on mean and variance features extracted from the three RGB channels. Then, a probabilistic neural network (PNN) was trained to classify test samples. Authors in [12] have considered different color, shape and texture features to classify seven date cultivars, where k-nearest neighbors (KNN) and linear discriminant analysis (LDA) along with Artificial Neural Network (ANN) were employed to perform classification. In [13], four types of date fruit from Saudi Arabia, namely Mabroom, Sukkary, Sagai and Ajwa, were classified based on different color and texture features. In [14], image is first decomposed into its color components, then, Weber Law descriptor (WLD) and Local Binary Patterns (LBP) are applied to each component to encode the texture of the date fruit. Indeed, the use of texture descriptors is somewhat convenient because texture of date fruit can differ according to the maturity degree of this fruit. Authors in [15] suggest using a Gaussian Mixture Model (GMM) to encode different visual appearances of date fruit e.g., each visual appearance corresponds to a maturity degree. Results of this work is then improved by including an outlier removal component in the classification pipeline to remove defective samples [7].

More recently, with the impressive performance achieved by deep-based approaches, several literature works have considered using deep learning-based schemes for classifying date fruit. As instance, in [16], pre-trained CNN models, including MobileNet and InceptionNet, were considered to classify six date varieties namely Ajwa, Boroy, Medjool, Moriam, Sokire and Sugaey. Similarly, an experimental comparative study was conducted to compare pre-trained CNN models for the classification of five types of date, where ResNet-50 has outperformed the remaining networks [17]. Similarly, in [8], a customized CNN is proposed to clas-

sify nine date varieties including Ajwa, Galaxy, Medjool, Meneifi, Nabat Ali, Rutab, Shaishe, Sokari and Sugaey. Authors in [18] have focused their attention on classifying the three most grown date types in Pakistan namely Assel, Karbalain and Kupro. Aiming to improve user satisfaction in smart cities, deep CaffeNet was employed to distinguish four types of date fruit in [19].

As for the second category of works, it comprises methods concerned with date grading based on maturity level. For instance, in [20], image of date fruit is firstly segmented based on a specific threshold, then, different morphological features, involving area and perimeter, were extracted to describe the date sample. A baseline condition-based approach was then employed to determine the maturity stage to which the test sample belongs, where Rutab, Kimri, Khalal and Tamer stages were considered. Authors in [21] have classified date samples, on the basis of ripeness level, into raw, under-ripe and ripe. Similarly, a machine vision system was developed by [22] to grade Berhee variety into three maturity stages. This system is composed of a conveying unit, illumination and capturing unit, and sorting unit, where each unit is designed to perform a particular role in the grading process. To handle the problem of labeled data scarcity, a dataset of different sizes and maturity stages of Medjool dates was introduced in [23].

Some other works have considered using CNN for date grading into different maturity degrees. As instance, an intelligent harvesting decision CNN-based system for detecting maturity level of date fruit was proposed in [24]. In this work, date samples were classified into seven different maturity levels from immature to Tamar stage. Similarly, to detect the Tamar stage of Medjool variety, several pre-trained CNN models, including VGG-16, VGG-19, ResNet-50, and AlexNet, were evaluated in [5]. This study pointed out that VGG-19 network can be used for building a vision system for Medjool grading. It is worth noting that some studies have considered date type classification and maturity stage detection at the same time. Representative works include the ones in [6] and [25], where the both have adopted a deep learning framework for date classification and sorting.

The third category of methods aim at inspecting the quality of date fruit e.g., detect the defective samples. For instance, authors in [3] proposed a method for discriminating healthy date samples (Shahani variety) from the defective ones using a modified version of VGG-16 network. In [26], date samples were categorized into good and sugar-defected categories using Bag Of Features (BOF). A Back Propagation Neural Networks (BPNN) is utilized to categorize dates into three classes by relying on the percentage of cracks within samples surface [4]. Handcrafted approaches were also used for determining the quality of date fruit. As instance, to grade dates into hard, semi-hard and soft, Linear discriminate analysis (LDA) and stepwise discriminate analysis (SDA) were used in [27]. To deal with the problem of limited number of labeled images, authors in [28] suggested using an evolution-

**TABLE 1. Number of date fruit samples per variety in our dataset.**

Date variety	Number of samples
Ajina	85
Adam Deglet Nour	86
Ghars	88
Litima	85
Bayd Hmam	87
Deglet kahla	85
Bouaalous	82
Degla bayda	95
Deglet ghabia	35
Dfar l gat	86
Dgoul	103
Tarmount	83
Tanslit	85
Deglet	38
Tantbucht	76
Techbeh Tati	88
Tivisyauin	87
Tinisin	88
Loullou	81
Hamraya	76

ary algorithm along with an AdaBoost training procedure to check the quality of date fruit. In [29], a hand-designed basic color and shape features were utilized to classify dates into three classes of quality namely class A, B and C. In another research [30], Mozafati dates were classified, based on length and freshness parameters, into different categories, from very poor to the excellent quality.

### III. DATE FRUIT DATASET COLLECTION

To assess the performance of proposed method, we introduce a new challenging dataset that is made up of 1619 images from twenty (20) different date varieties. These varieties are Ajina, Adam Deglet Nour, Bayd Hmam, Bouaalous, Deglet, Deglet kahla, Deglet ghabia, Degla bayda, Dfar l gat, Dgoul, Ghars, Litima, Loullou, Hamraya, Tarmount, Tanslit, Tantbucht, Techbeh Tati, Tivisyauin and Tinisin. The number of samples per variety is shown in Table 1. Date samples are collected from local markets of Touggourt region located in the south of Algeria. Note that some varieties are not available throughout the year, but they appear in specific months in the year. For instance, Tantbucht variety is available only during the months of September and October every year. Images were taken using a camera at a resolution of  $4128 \times 3069$  pixels. These varieties may differ from each other in terms of flavor, shape, size, color, maturity level and hardness degree. However, there exists some varieties that highly resemble each other e.g., Litima and Bayd Hmam, which makes it difficult to distinguish them FIGURE 1 presents typical samples from each variety, and FIGURE 2 shows different maturity levels for certain varieties. Note that the dataset is publicly available at <https://unsat.000webhostapp.com/dataset>.



**FIGURE 1.** From top to bottom and from left to right, displayed date varieties are Ajina, Adam Deglet Nour, Bayd Hmam, Bouaarous, Deglet, Deglet kahla, Deglet ghabia, Degla bayda, Dfar lgat, Dgoul, Ghars, Litima, Loullou, Hamraya, Tarmount, Tanslit, Tantbucht, Techbeh Tati, Tivisyauin and Tinisin.



**FIGURE 2.** Date samples in different maturity levels (leftmost: immature, at center: semi-mature and rightmost: mature). From top to bottom, names of varieties are Adam Deglet Nour, Hamraya, Tanslit and Tinisin.

**IV. PROPOSED METHOD**

The general pipeline of the date fruit sorting process is depicted in FIGURE 3, and the proposed method is illustrated by the block diagram shown in FIGURE 4. As can be seen from FIGURE 4, our proposed method consists of two stages which are training and testing. In the first stage, we extract features from date fruit images using both unsupervised and supervised deep networks (PCANet and VGG-F, respectively). Then, to improve the classification outcomes, we consider using discriminant correlation analysis (DCA)

method for combining both types of features. To perform classification, the K-nearest neighbor classifier (KNN) is used to classify the different varieties. Hereafter, we provide details on the proposed method.

**A. SUPERVISED CONVOLUTIONAL NEURAL NETWORK ARCHITECTURE**

Due to their excellent performance, pre-trained CNNs have been widely used in several computer vision tasks [31], [32].

In the literature, there are various pre-trained architectures of CNN which have been trained on large-scale image databases. In particular, ImageNet, which contains 1000 different classes, has been used to train the dominant CNN architectures such as VGG-16, VGG-19, ResNet, GoogleNet... etc. In fact, each of these architectures has its specifications i.e., number of layers and parameters, and order of layers. Existing works on date fruit sorting consider two strategies in exploiting pre-trained networks. The first strategy is to fine-tune the network on the training part of the dataset being classified. In the second one, features are extracted from the last layers and then fed to a conventional classifier. According to [33], the CNN depth is a crucial factor in determining the quality of classification results. Therefore, we opt for using VGG-F [34], as its depth is enough to extract representative features from date fruit images. Another reason behind the selection of this network is that a CNN with a small depth takes less processing time compared to the ones with a higher depth. The architecture of VGG-F is presented in Table 2.





FIGURE 3. The pipeline of the date fruit sorting process: 1) Date fruit harvesting and image acquisition, 2) features extraction and classification, and 3) different classification outcomes.

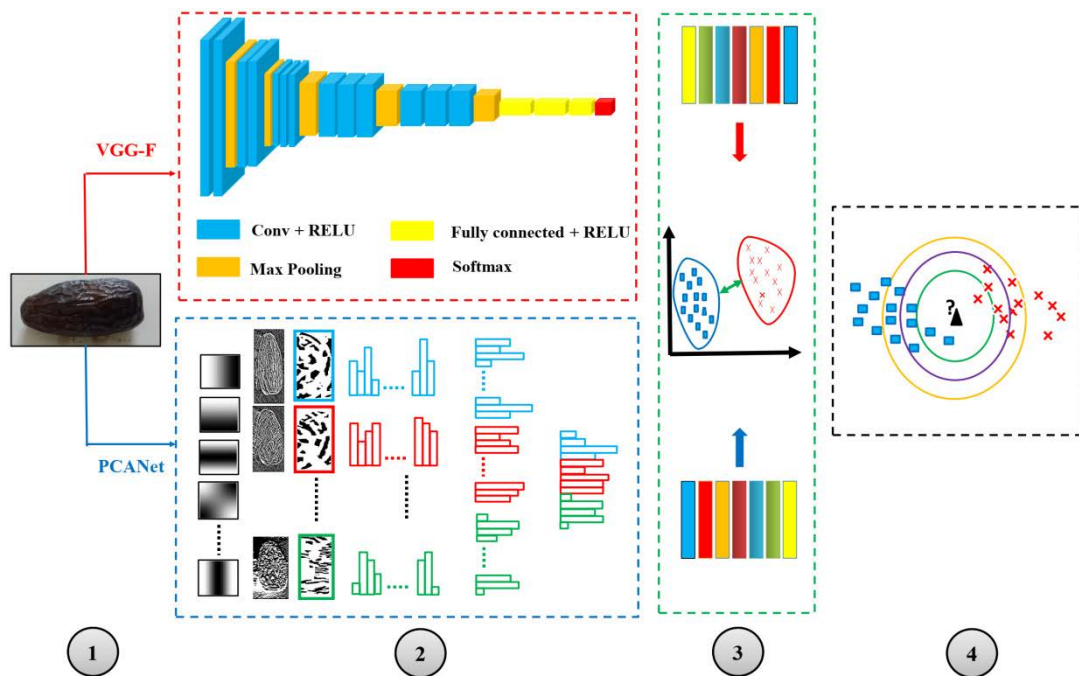


FIGURE 4. The general flowchart of the proposed method: 1) input date fruit image, 2) features extraction using supervised network (VGG-F) and unsupervised network (PCANet), 3) features fusion using DCA and 4) classification using KNN classifier.

### B. UNSUPERVISED DEEP NEURAL NETWORK ARCHITECTURE

As an unsupervised deep network, we opt for a computationally fast method called PCANet [35], which is an efficient deep learning architecture that is capable to generate reliable representations from date fruit images. PCANet is composed of several successive layers, starting by filter bank generation

and ending by block-wise histogramming. Hereafter, we give more details on this method by explaining each of its steps separately.

#### 1) FILTER BANK GENERATION

Suppose we have a training set of  $N$  images of size  $m \times n$ , which is referred to as  $\{Tr_i\}$ , such that  $i = 1, \dots, N$ . For

TABLE 2. Architecture of pre-trained VGG-F network.

Layer	Filter	Stride	Output size
Conv. 1	$11 \times 11$	4	$109 \times 109 \times 64$
Relu. 1			$109 \times 109 \times 64$
Norm. 1			$109 \times 109 \times 64$
Pool. 1	$3 \times 3$	2	$54 \times 54 \times 64$
Conv. 2	$5 \times 5$	1	$26 \times 26 \times 256$
Relu. 2			$26 \times 26 \times 256$
Norm. 2			$26 \times 26 \times 256$
Pool. 2	$3 \times 3$	2	$13 \times 13 \times 256$
Conv. 3	$3 \times 3$	1	$13 \times 13 \times 256$
Relu. 3			$13 \times 13 \times 256$
Conv. 4	$3 \times 3$	1	$13 \times 13 \times 256$
Relu. 4			$13 \times 13 \times 256$
Conv. 5	$3 \times 3$	1	$13 \times 13 \times 256$
Relu. 5			$13 \times 13 \times 256$
Pool. 5	$3 \times 3$	2	$6 \times 6 \times 256$
Fc. 6			$4096 \times 1$
Relu. 6			$4096 \times 1$
Fc. 7			$4096 \times 1$
Relu. 7			$4096 \times 1$
Fc. 8			$1000 \times 1$

computation purposes, we consider a  $p_1 \times p_2$  patch around every pixel. All patches are collected from  $Tr^i$  and then vectorized, where patches of the  $i^{th}$  image are denoted by  $x_{i,1}, x_{i,2}, \dots, x_{i,\tilde{m},\tilde{n}}$ , and  $\tilde{m} = m - \lfloor \frac{p_1}{2} \rfloor$ ,  $\tilde{n} = n - \lfloor \frac{p_2}{2} \rfloor$ ,  $\lfloor b \rfloor$ , and  $\lfloor b \rfloor$  stands for the smallest integer  $\geq b$ . By subtracting the patch mean from each patch, we obtain.  $\tilde{X}_i = [\tilde{x}_{i,1}, \tilde{x}_{i,2}, \dots, \tilde{x}_{i,\tilde{m},\tilde{n}}]$ . The same matrix is constructed for all the images and fused together as follows

$$X = [\tilde{X}_1, \tilde{X}_2, \dots, \tilde{X}_N] \quad (1)$$

PCA aims at finding an orthogonal matrix that minimizes the reconstruction error, such that number of filters is set to  $M$ , this can be achieved as follows:

$$\min_{V \in \mathbb{R}^{p_1 \times p_2 \times M}} \|X - VV^T X\|_F^2 \quad s.t. \quad VV^T = I_M \quad (2)$$

where  $I_M$  and  $V$  stand for the unit matrix of size  $M \times M$  and the standard orthogonal matrix, respectively. PCA is calculated on the set  $X$  to extract the principal eigenvectors, which are then ordered in descending way according to their respective eigenvalues. PCA filters are then generated by reconstructing the top  $M$  principal eigenvectors, as given by

$$W_k = mat_{p_1,p_2}(q_k(XX^T)) \in \mathbb{R}^{p_1 \times p_2}, \quad k = 1, 2, \dots, M \quad (3)$$

where  $j^{th}$  is the  $j^{th}$  PCA filter, is the covariance matrix of  $X$ ,  $q_k()$  extracts the principal eigenvectors from the covariance matrix, and  $mat_{p_1,p_2}()$  is a function that maps a vector  $v \in \mathbb{R}^{p_1 \times p_2}$  to a matrix  $W \in \mathbb{R}^{p_1 \times p_2}$ . FIGURE 5 presents some filters that are learned using the PCA.

## 2) CONVOLUTION LAYER

This first layer in the network acts as a feature detector. Each image in  $\{Tr_i\}$  is convolved using the filters learned in the

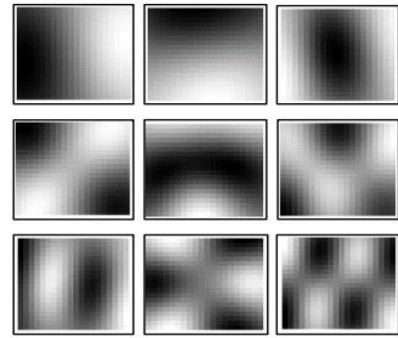


FIGURE 5. Typical filters learned using PCA.

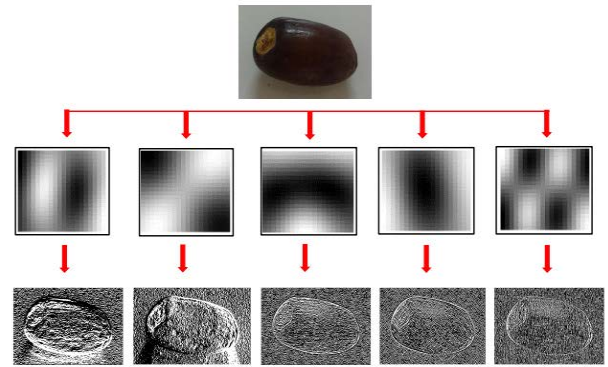


FIGURE 6. Typical results of convolution performed using learned filters.

previous step. Note that the boundary of  $Tr^i$  is zero-padded to have an output image (called  $C_i$ ) having the same size as  $Tr^i$ . Convolution is performed according to the next equation

$$C_i = Tr^i * W_k, \quad i = 1, \dots, N, \quad k = 1, \dots, M \quad (4)$$

such that  $W_k$  represents the set of PCA filters. FIGURE 6 presents the results of convolving a date fruit image with some filters from the PCA filter bank. A second convolution layer can be considered to extract deeper features. As this second layer increases the processing time significantly, in this work we consider the first layer only [36].

## 3) BINARY HASHING AND BLOCK-WISE HISTOGRAMMING

The main target of binary hashing process is to discriminate the pixel's responses to the PCA filters. The outputs of convolution layer are real-valued feature maps, thus, each of which is binarized according to the following formula

$$BIN(C^i) = \begin{cases} 1, & \text{if } C^i > 0 \\ 0, & \text{otherwise} \end{cases} \quad (5)$$

After binarizing each feature map separately, they are combined into a single image (denoted by  $O^i$ ), according to the following equation

$$O^i = \sum_{r=1}^M 2^{r-1} \times BIN(C^r) \quad (6)$$

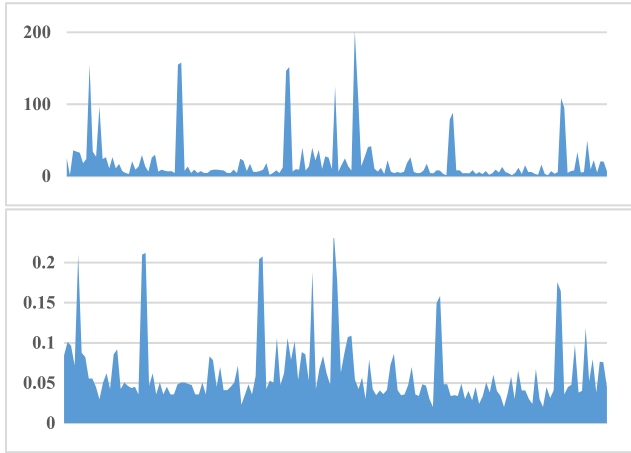


**FIGURE 7.** Histogram before (top) and after (bottom) performing the normalization.

As a consequence, every pixel in  $O^i$  ranging from 0 to  $2^M - 1$ . Therefore, a histogram that counts the appearance frequency of every value in this range is generated. To take advantage of spatial relationship,  $O^i$  is divided into  $B$  non-overlapping blocks, and a histogram, denoted as  $H_b$  ( $b = 1, \dots, B$ ) is extracted from each block. The final histogram is formed by combining the local histograms extracted from different blocks.

#### 4) HISTOGRAM NORMALIZATION

Indeed, this last step is not included in the original PCANet, but we include it for two reasons. First, to get rid of the negative influence of illumination changes among different date samples. Second, this normalization makes the histogram more evenly distributed (see FIGURE 7), and relieve the disparity of visual features. Note that a significant disparity of features can dramatically distort the classification outcomes. To perform normalization, we consider power- $L_2$  rule. For a histogram  $H = (h_1, \dots, h_f)$ , power- $L_2$  rule is given by

$$h_i = \frac{|h_i|^\beta}{\|H\|} \quad (7)$$

$\|H\|$  is the  $L_2$  norm of  $H$ , and  $\beta$  is a constant, such that  $0 \leq \beta \leq 1$ .

### C. FEATURE FUSION USING DISCRIMINANT CORRELATION ANALYSIS

In order to improve the individual decisions achieved by each of supervised and unsupervised deep networks, we consider incorporating them at feature level. To do so, we employ the discriminant correlation analysis (DCA) technique [37].

The principle of DCA is to maximize the pairwise correlations in the two different feature sets by jointly removing the inter-class correlations and limiting the correlations to be intra-classes. One interesting advantage of DCA is its low computational complexity, which makes it possible to integrate it in real-time systems. Another point is that DCA can

be thought as features reduction technique because, in most cases, features yielded upon fusion have lower dimensions compared to the original features.

More formally, let us consider a set of training images of  $k$  classes, which is denoted by  $E = \{(x_1, y_1), (x_2, y_2), \dots, (x_n, y_n)\}$ , where  $y_i = \{1, \dots, k\}$  is the class for which a specific image  $x_i$  belongs. We denote by  $X_1$  and  $X_2$  the features extracted from the training set using supervised and unsupervised networks, respectively. The first step is to calculate mean of each class and the overall mean of the training set using (8) and (9), respectively.

$$\bar{x}_i = \frac{1}{m_i} \sum_{j=1}^{m_i} x_j^i \quad (8)$$

where  $m_i$  is the number of date samples in the  $i^{\text{th}}$  class.

$$\bar{x} = \frac{1}{n} \sum_{v=1}^k m_v \bar{x}_v \quad (9)$$

The second step is the calculation of the covariance matrix, which can be done as follows

$$\text{Sigma} = \Phi^T \Phi \quad (10)$$

where  $\Phi = \sqrt{m_1}(\bar{x}_1 - \bar{x}), \dots, \sqrt{m_k}(\bar{x}_k - \bar{x})$ .

Then, singular value decomposition of  $\text{Sigma}$  is computed as follows

$$\text{Sigma} = U \Lambda U^T \quad (11)$$

Such that  $\Lambda = \text{Diag}(\lambda_1, \lambda_2, \dots, \lambda_k)$ , here  $\lambda_i$  is the  $i^{\text{th}}$  eigenvalue of  $\text{Sigma}$ , and the  $i^{\text{th}}$  column of  $U$  is its respective eigenvector. Note that eigenvalues are ordered in a decreasing order. By considering the top  $t$  eigenvalues and their respective eigenvectors, the transformation matrix is given by

$$R = \Phi U_t \Lambda_t^{-1/2} \quad (12)$$

The above steps are performed on each of  $X$  and  $X_2$  separately. After having the transformation matrix calculated, data-points are transformed accordingly as follows:

$$Z_1 = R^T X_1, \quad Z_2 = R^T X_2 \quad (13)$$

The next step is to calculate the between-set covariance matrix of the transformed features, as (14)

$$S_b = Z_1 Z_2^T \quad (14)$$

Afterwards, the SVD of  $S_b$  is calculated using (15)

$$S_b = \sqrt{\sum V^T} \quad (15)$$

Then, the transformation matrix is given by

$$T = \sqrt{\sum^{-1/2}} \quad (16)$$

According to the transformation matrix  $T$ , transformed data is generated as follows

$$X'_1 = T^T Z_1, \quad X'_2 = T^T Z_2 \quad (17)$$

**TABLE 3.** The subsets of parameters that are considered.

Subset of parameters	Number of filters for PCA	Filter size	Block size
1	8	5 × 5	50 × 50
2	7	7 × 7	32 × 32
3	9	9 × 9	22 × 22
4	5	7 × 7	100 × 100
5	6	9 × 9	22 × 22

**TABLE 4.** Performance of the different subsets of PCANet using the three classifiers (± stands for the standard deviation).

Subset of parameters	SVM	DT	KNN
1	91.72±0.002	81.32±0.018	95.12±0.003
2	92.03±0.006	81.74±0.025	<b>95.48±0.005</b>
3	87.34±0.014	74.54±0.008	94.37±0.002
4	92.95±0.005	83.15±0.017	92.09±0.004
5	91.73±0.013	76.67±0.023	94.31±0.004

Finally, output features are generated according to the next equation

$$X' = X'_1 + X'_2 \tag{18}$$

**D. CLASSIFICATION MODEL**

After having visual features of the dataset generated, a last step is to classify the test samples. To this end, we consider using three different classifiers namely K-nearest neighbor (KNN), Support vector machine (SVM) and decision trees (DT).

**V. EXPERIMENTS AND DISCUSSION**

This section is devoted to evaluate the performance of the proposed method. To do so, we conduct multiple experiments, each of which is intended to measure a specific aspect in the proposed method. Experiments are carried out on our dataset described in Section 3. Regarding data splitting, we consider using a 3-fold cross validation procedure, where, in each iteration, 2 folds are employed for training and one fold is intended for testing.

**A. EXPERIMENTAL RESULTS**

**1) EFFECT OF PARAMETERS ON THE PERFORMANCE OF PCANET**

The target of this experiment is to detect the parameters subset that maximizes the classification performance of PCANet. PCANet requires three main parameters which are the number of filters, filter size and block size. Thus, we have evaluated five subsets as shown by Table 3. We report the performance of different subsets using the three classifiers i.e., KNN, DT and SVM.

Table 4 presents the classification accuracy for the five subsets of parameters using the three classifiers. The first thing to note is the disparity between the performance of different

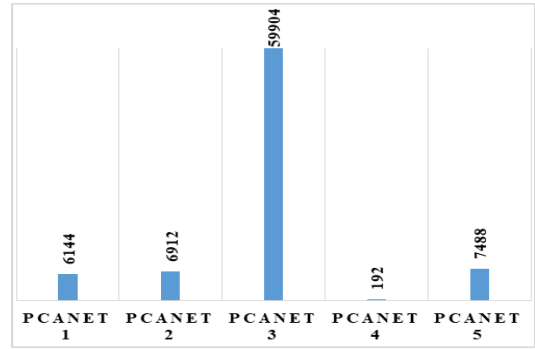


**FIGURE 8.** Dimension of features extracted using the different subsets of PCANet parameters.

subsets when using different classifiers. It can be noted that compared to other classifiers, KNN has achieved the best performance in most of the subsets. For instance, the highest score is reached by the second subset with KNN (95.48%). Even though it takes a considerable time for training, we can notice that DT has achieved a minor performance compared to KNN and SVM classifiers (the best score is for the DT is 83.15%). In addition, one can see the close relationship between the feature dimensions and performance of the SVM and DT (FIGURE 8 shows the features dimension of the different subsets). For instance, SVM and DT has achieved the least performance (87.34% and 74.54 %, respectively) when dealing with high dimensional feature vectors. In the contrary, the performance of the KNN classifier is not consistent with this last observation, as the least performance of KNN (92.09%) has been scored with the lower dimensional feature vectors (192 dimensions). Regarding the values of the standard deviation, we can see that they are close to zero, which means that the accuracy yielded by the three folds is roughly the same.

As for the effect of the PCANet parameters (i.e., number of filters, filter and block size), we can notice that the first parameter has significant influence on the overall performance of the method. This is explained by the fact that by rising the number of filters, the dimension of feature vector increases exponentially (dimension of local histograms is equal to the number of filter power of two). Therefore, this parameter should be a compromise between the number of filters and feature vector dimension. In our case, we can see that using seven filters is enough to achieve a good performance (92.03% for SVM, 81.74% for DT and 95.48% for KNN). As for the filter size, the employed filters have to be large enough to capture spatial features of date fruit. Nevertheless, too large filters can cause losing some minor details that could considerably improve the final decisions. Furthermore, the block size parameter is incorporated to provide spatial relationship information which can boost the classification outcomes.

This parameter has also influence on feature dimension (and thus the classification results) because the final feature



**TABLE 5.** Performance of VGG-F layers et using the three classifiers ( $\pm$  stands for the standard deviation).

VGG-F layer	SVM	DT	KNN
Conv. 2	91.16 $\pm$ 0.015	88.35 $\pm$ 0.024	84.11 $\pm$ 0.024
Conv. 3	91.77 $\pm$ 0.018	93.14 $\pm$ 0.004	89.36 $\pm$ 0.014
Conv. 4	91.84 $\pm$ 0.009	93.64 $\pm$ 0.006	90.23 $\pm$ 0.014
Conv. 5	91.59 $\pm$ 0.006	92.51 $\pm$ 0.006	89.68 $\pm$ 0.013
Fc. 6	93.33 $\pm$ 0.007	92.84 $\pm$ 0.012	93.21 $\pm$ 0.008
Fc. 7	94.80 $\pm$ 0.007	92.40 $\pm$ 0.008	<b>94.81<math>\pm</math>0.009</b>
Fc. 8	94.30 $\pm$ 0.007	91.90 $\pm$ 0.005	94.25 $\pm$ 0.004

**TABLE 6.** Accuracies achieved by combining different PCANet versions and VGG-F layers using DCA and SVM ( $\pm$  stands for the standard deviation).

VGG-F layer	Subset 1	Subset 2	Subset 3
Conv. 2	95.62 $\pm$ 0.006	95.11 $\pm$ 0.005	94.13 $\pm$ 0.006
Conv. 3	96.17 $\pm$ 0.0007	96.28 $\pm$ 0.005	95.05 $\pm$ 0.005
Conv. 4	96.66 $\pm$ 0.003	96.53 $\pm$ 0.006	95.54 $\pm$ 0.004
Conv. 5	96.35 $\pm$ 0.004	96.29 $\pm$ 0.006	95.73 $\pm$ 0.004
Fc. 6	97.39 $\pm$ 0.007	97.27 $\pm$ 0.006	97.33 $\pm$ 0.004
Fc. 7	97.83 $\pm$ 0.004	97.76 $\pm$ 0.009	<b>98.20<math>\pm</math>0.003</b>
Fc. 8	97.83 $\pm$ 0.004	97.33 $\pm$ 0.008	97.65 $\pm$ 0.002

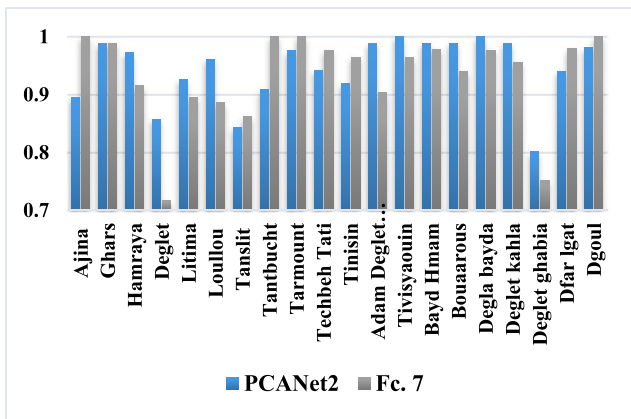


**FIGURE 9.** Performance per variety reached by each of Fc.7 and PCANet (subset 2).

vector is formed by concatenating local histograms. In this experiment, considering a block size of  $32 \times 32$  appears to be a good compromise for the three classifiers.

2) PERFORMANCE OF DIFFERENT CNN LAYERS

Each layer within CNN (VGG-F in our case) yields classification results that differ from the results obtained by the remaining layers. Therefore, we report the performance of each layer in VGG-F separately. This can help determining the layer that can better capture the features extracted using the PCANet. Table 5 reports the classification accuracy of each layer in the network using SVM, DT and KNN.

From Table 5, when using SVM and KNN, it can be seen that, as expected, later layers have achieved better accuracy than the earlier layers. Typically, early layers encode low-level features, whereas late layers encode object-specific characteristics and involve more semantic information. Among the different layers, the fully connected layer (Fc. 7) has scored the highest accuracy compared to the remaining layers (94.8% using SVM and 94.81% using KNN). However, it can be noticed that the performance of different layers is comparable when using the DT classifier. To get more insights on those results, we report the performance per variety of Fc. 7 along with PCANet (subset2) using the KNN classifier (see FIGURE 9).

From FIGURE 9, we remark that PCANet and Fc. 7 outperformed each other interchangeably. For instance, PCANet scored an accuracy of 89.48% in Ajina variety, whereas, Fc.7 has surpassed this rate and achieved an accuracy of 100%. However, PCANet has classified samples of Deglet variety much better than Fc. 7 (85.78% and 71.71%, respectively). This disparity in performance is promising and encourages investigating the complementarity of both kind of features. Indeed, by inspecting the classification results, we can see that 4 out of 20 varieties (Ajina, Tanttucht, Tarmount and Dgoul) were achieved a perfect classification accuracy of 100% using the Fc. 7, whereas, 2 varieties (Tivisyauin and Degla Bayda) have reached 100% using the PCANet. If we look at the Ajina variety, we can see that it is relatively easy to be distinguished due to its size, color and shape. However, what is actually surprising is to successfully classify all the samples of Dgoul variety which strongly resemble many varieties such as Tinisin and Tanslit.

3) RESULTS OF FUSING SUPERVISED AND UNSUPERVISED NETWORKS

After reporting the individual performance of each of supervised VGG-F and unsupervised PCANet, we provide details on the results obtained by combining the both networks. According to the previous experiment, it has been shown the significant disparity of results yielded by each network. In this case, fused features could achieve promising results. Therefore, we fuse features learned from the two networks using DCA technique. We compare the performance of the DCA with canonical correlation analysis (CCA) [38] algorithm in terms of classification accuracy, features dimension and processing time.

a: FUSION PERFORMANCE USING DISCRIMINANT CORRELATION ANALYSIS (DCA)

At first, we report the classification accuracy yielded by combining each layer from VGG-F with the three first PCANet subsets (i.e., subset 1, subset 2 and subset 3) using the DCA. We limit our attention on the first three subsets as their performance is similar to the performance of the remaining subsets (i.e., subset 4 and 5). Table 6, 7 and 8 report the fusion results using SVM, DT and KNN, respectively.

**TABLE 7. Accuracies achieved by combining different PCANet versions and VGG-F layers using DCA and DT ( $\pm$  stands for the standard deviation).**

VGG-F layer	Subset 1	Subset 2	Subset 3
Conv. 2	85.88 $\pm$ 0.028	87.59 $\pm$ 0.006	86.85 $\pm$ 0.007
Conv. 3	88.27 $\pm$ 0.012	88.25 $\pm$ 0.005	89.55 $\pm$ 0.010
Conv. 4	87.96 $\pm$ 0.007	89.80 $\pm$ 0.006	88.87 $\pm$ 0.007
Conv. 5	87.34 $\pm$ 0.015	89.19 $\pm$ 0.013	87.89 $\pm$ 0.001
Fc. 6	92.33 $\pm$ 0.006	92.47 $\pm$ 0.009	91.92 $\pm$ 0.017
Fc. 7	92.91 $\pm$ 0.016	<b>93.09<math>\pm</math>0.010</b>	92.53 $\pm$ 0.011
Fc. 8	92.83 $\pm$ 0.004	92.22 $\pm$ 0.003	90.94 $\pm$ 0.021

**TABLE 8. Accuracies achieved by combining different PCANet versions and VGG-F layers using DCA and KNN ( $\pm$  stands for the standard deviation).**

VGG-F layer	Subset 1	Subset 2	Subset 3
Conv. 2	94.14 $\pm$ 0.016	93.40 $\pm$ 0.013	92.58 $\pm$ 0.006
Conv. 3	95.93 $\pm$ 0.008	94.30 $\pm$ 0.015	94.50 $\pm$ 0.009
Conv. 4	96.10 $\pm$ 0.008	94.92 $\pm$ 0.015	95.17 $\pm$ 0.003
Conv. 5	96.17 $\pm$ 0.007	94.86 $\pm$ 0.007	94.86 $\pm$ 0.008
Fc. 6	97.09 $\pm$ 0.003	96.04 $\pm$ 0.005	96.28 $\pm$ 0.005
Fc. 7	97.09 $\pm$ 0.004	85.50 $\pm$ 0.201	95.39 $\pm$ 0.032
Fc. 8	<b>97.40<math>\pm</math>0.003</b>	95.62 $\pm$ 0.013	94.53 $\pm$ 0.037

As can be seen from Table 6, 7 and 8, combining features computed using different CNN layers with different variants of PCANet yields distinct accuracies. The first observation we can make is that consider fusing later layers of the VGG-F network yields, in most cases, than considering the earlier layers. This is because the depth of the earlier layers is not enough to capture the characteristics of different date fruit varieties. We can notice that by using SVM all the accuracies reached by the fused features are better than accuracies of individual features. For instance, each of subset 1 and Fc.7 have scored an accuracy of 91.72% and 94.8%, respectively, whereas fusing those two features using DCA yields an overall accuracy of 97.83%. Regarding the performance of DCA with the KNN classifier, we can notice that combining the VGG-F layers with subsets 1 and 3 improves the individual performance in most cases, while, most combinations in which subset 2 is considered the accuracy prior to fusion was better than the accuracy obtained by fusion. Another thing to note is that results obtained by the DT classifier after performing features fusion were minor than the individual results. We can also that the values of the standard deviation are close to zero, which means that the accuracy achieved by the three folds is roughly the same. In general, the highest accuracy (98.20%) is obtained by fusing Fc. 7 and subset 3 using SVM. Among the three classifiers, the experiments reveal that the SVM is the most suitable for this task. For a comprehensive analysis, we report the performance per variety for the best combination using DCA i.e., Fc. 7 and subset 3 (FIGURE 10). As can be seen from FIGURE 10, in most varieties, the combination of Fc. 7 and subset 3 outscored the

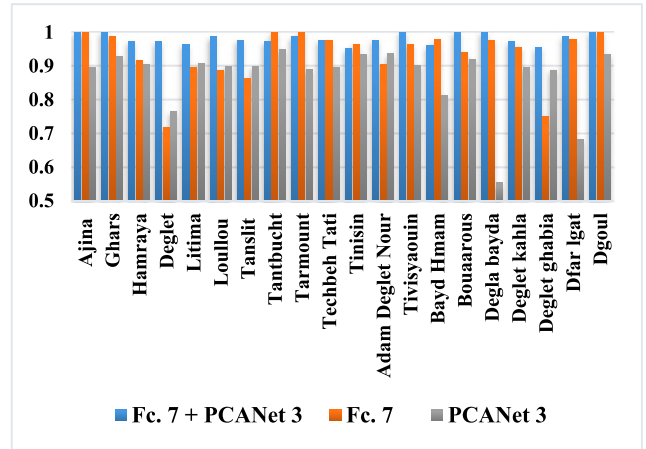


**FIGURE 10. Accuracy per variety for the best combination (Fc. 7 + PCANet 3) using the DCA and SVM.**

**TABLE 9. Accuracies achieved by combining different PCANet versions and VGG-F layers using CCA and SVM ( $\pm$  stands for the standard deviation).**

VGG-F layer	Subset 1	Subset 2	Subset 3
Conv. 2	98.70 $\pm$ 0.005	98.64 $\pm$ 0.007	98.15 $\pm$ 0.004
Conv. 3	99.26 $\pm$ 0.003	<b>99.32<math>\pm</math>0.004</b>	99.01 $\pm$ 0.005
Conv. 4	99.01 $\pm$ 0.003	99.01 $\pm$ 0.005	99.07 $\pm$ 0.005
Conv. 5	99.01 $\pm$ 0.004	99.01 $\pm$ 0.007	98.89 $\pm$ 0.006
Fc. 6	99.07 $\pm$ 0.006	99.07 $\pm$ 0.004	99.01 $\pm$ 0.004
Fc. 7	99.01 $\pm$ 0.006	99.19 $\pm$ 0.003	98.88 $\pm$ 0.003
Fc. 8	99.13 $\pm$ 0.003	98.88 $\pm$ 0.006	98.82 $\pm$ 0.007

**TABLE 10. Accuracies achieved by combining different PCANet versions and VGG-F layers using CCA and DT ( $\pm$  stands for the standard deviation).**

VGG-F layer	Subset 1	Subset 2	Subset 3
Conv. 2	55.47 $\pm$ 0.010	58.55 $\pm$ 0.024	56.39 $\pm$ 0.064
Conv. 3	61.42 $\pm$ 0.031	61.51 $\pm$ 0.022	<b>65.04<math>\pm</math>0.027</b>
Conv. 4	60.54 $\pm$ 0.037	63.71 $\pm$ 0.022	63.82 $\pm$ 0.022
Conv. 5	57.46 $\pm$ 0.022	58.71 $\pm$ 0.039	59.91 $\pm$ 0.022
Fc. 6	64.40 $\pm$ 0.043	60.71 $\pm$ 0.022	61.87 $\pm$ 0.058
Fc. 7	63.03 $\pm$ 0.086	60.00 $\pm$ 0.093	60.02 $\pm$ 0.066
Fc. 8	60.33 $\pm$ 0.041	53.80 $\pm$ 0.079	51.84 $\pm$ 0.039

individual performance of each network. This demonstrates the complementarity of those networks.

*b: FUSION PERFORMANCE USING CANONICAL CORRELATION ANALYSIS (CCA)*

In this experiment, we report the performance of the proposed method when considering the canonical correlation analysis CCA instead the DCA. Table 9, 10 and 11 present the results of fusing each layer from the VGG-F and the three subsets of the PCANet using the CCA, where classification is performed using SVM, DT and KNN, respectively.

As a first remark, we can notice that fusion results using SVM is nearly optimal for the most of combinations. For

**TABLE 11.** Accuracies achieved by combining different PCANet versions and VGG-F layers using CCA and KNN ( $\pm$  stands for the standard deviation).

VGG-F layer	Subset 1	Subset 2	Subset 3
Conv. 2	89.01 $\pm$ 0.006	91.53 $\pm$ 0.001	90.98 $\pm$ 0.004
Conv. 3	92.77 $\pm$ 0.001	94.00 $\pm$ 0.001	93.70 $\pm$ 0.003
Conv. 4	93.32 $\pm$ 0.007	<b>94.31<math>\pm</math>0.005</b>	94.30 $\pm$ 0.006
Conv. 5	93.26 $\pm$ 0.003	94.25 $\pm$ 0.0009	93.39 $\pm$ 0.005
Fc. 6	90.92 $\pm$ 0.014	92.65 $\pm$ 0.004	91.73 $\pm$ 0.016
Fc. 7	90.94 $\pm$ 0.021	93.46 $\pm$ 0.016	92.28 $\pm$ 0.009
Fc. 8	90.06 $\pm$ 0.013	91.62 $\pm$ 0.023	90.62 $\pm$ 0.015

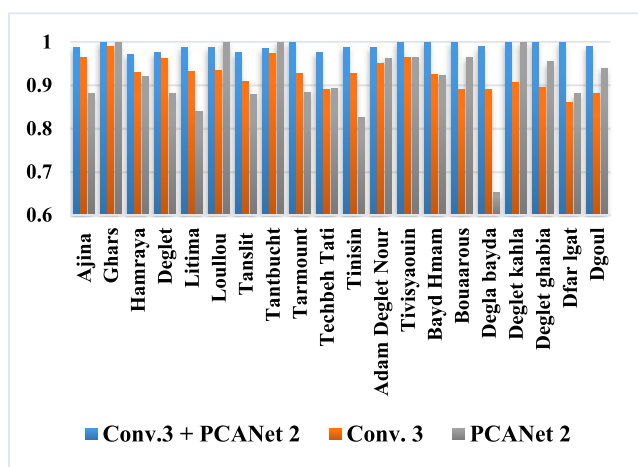


**FIGURE 11.** Accuracy per variety for the best combination (Conv. 3 + PCANet 2) using the CCA and SVM.

instance, combining the subset 2 with conv. 3 has yielded an accuracy of 99.32%. However, by using the DT and KNN classifiers the classification accuracies have been significantly decreased. FIGURE 11 reports the performance per variety for the best combination using CCA i.e., Conv. 3 and subset 2. From this figure, we can notice that different varieties achieve comparable high accuracies. We note also that the accuracy reached by fusing conv.3 and subset 2 is higher than the individual accuracy of the fused networks for all the varieties.

*c: COMPARISON OF DCA AND CCA*

The accuracy classification is not the only factor to consider for the assessment of feature fusion methods. Therefore, we consider comparing the CCA and DCA in terms of processing time and dimension of features after fusion. We report the dimension of features extracted from different CNN layers and the three variants of PCANet along with the features dimension after conducting the fusion using CCA and DCA (see FIGURE 12). From this figure, and by inspecting features dimension prior and after fusion, we can notice that dimension has significantly been reduced by using DCA because only top ranked eigenvalues are considered to construct the transformation matrix. For instance, the dimension

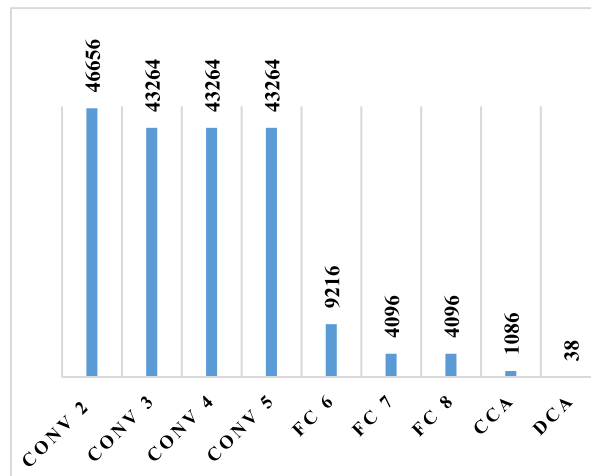


**FIGURE 12.** Dimension of features extracted using the different VGG-F layers and dimension of features fused using DCA and CCA.

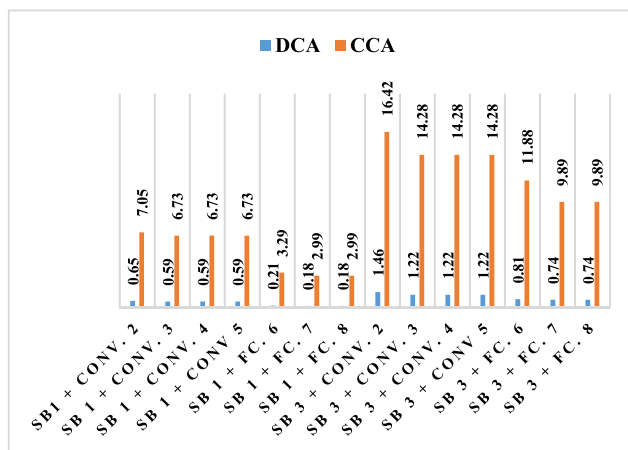


**FIGURE 13.** Processing time taken by each of DCA and CCA for the fusion of features extracted supervised (VGG-F) and unsupervised (PCANet) networks.

of features extracted from Fc. 6 and PCANet3 are 9216 and 59904, respectively, whereas, after performing feature fusion the dimension becomes 38, which is much less than initial dimensions. However, dimension of features after conducting fusion using CCA is 1086, which is much higher than dimension of features produced by the DCA. This makes the matching process using the features produced by the DCA faster and more efficient than using features produced using the CCA.

We also compare the processing time required to conduct each of DCA and CCA. We report the processing time taken by each of the two algorithms for the fusion of some pairs of supervised and unsupervised networks (see FIGURE 13, where time is computed in seconds).

From FIGURE 13, it evidently appears that CCA requires much more time than DCA. For instance, DCA requires only 0.65 seconds for fusing subset 1 and conv. 2, whereas, to do the same job, CCA takes 7.05 seconds. In average, the processing time required by the CCA is twelve times the processing time required by DCA. To conclude, in view

**TABLE 12.** Confusion matrix generated using the best combination (Fc. 7 + PCANet 3) obtained using DCA and SVM.

	1	2	3	4	5	6	7	8	9	10	11	12	13	14	15	16	17	18	19	20	
1	29	0	0	0	0	0	0	0	0	0	0	0	0	0	0	0	0	0	0	0	100%
2	0	30	0	0	0	0	0	0	0	0	0	0	0	0	0	0	0	0	0	0	100%
3	0	0	25	0	0	0	0	0	0	0	0	0	0	0	0	0	0	1	0	0	96%
4	0	0	0	13	0	0	0	0	0	0	0	0	0	0	0	0	0	0	0	0	100%
5	0	0	0	0	29	0	0	0	0	0	0	0	0	0	0	0	0	0	0	0	100%
6	0	0	1	0	0	26	0	0	0	0	0	0	0	0	0	0	0	0	0	0	96%
7	0	0	0	1	0	0	27	0	0	0	1	0	0	0	0	0	0	0	0	0	93%
8	0	0	0	0	0	0	0	26	0	0	0	0	0	0	0	0	0	0	0	0	100%
9	0	0	0	0	0	0	0	0	28	0	0	0	0	0	0	0	0	0	0	0	100%
10	0	0	0	0	0	0	0	0	0	30	0	0	0	0	0	0	0	0	0	0	100%
11	0	0	0	0	0	0	2	0	0	0	28	0	0	0	0	0	0	0	0	0	93%
12	0	0	0	0	0	0	0	0	0	0	0	29	0	0	0	0	0	0	0	0	100%
13	0	0	0	0	0	0	0	0	0	0	0	0	29	0	0	0	0	0	0	0	100%
14	0	0	0	0	0	0	0	0	0	0	0	0	0	29	0	0	0	0	0	0	100%
15	0	0	0	0	0	0	1	0	0	0	0	0	0	0	26	0	0	0	1	0	92%
16	0	0	0	0	0	0	0	0	0	0	0	0	0	0	0	32	0	0	0	0	100%
17	0	0	0	0	0	0	0	0	0	0	0	0	0	0	0	0	28	1	0	0	96%
18	0	0	0	0	0	0	0	0	0	0	0	0	0	0	0	0	0	12	0	0	100%
19	0	0	0	0	0	0	0	0	0	0	0	0	0	0	1	0	0	0	28	0	96%
20	0	0	0	0	0	0	0	0	0	0	0	0	0	0	0	0	0	0	0	35	100%

of the comparison results, where DCA and CCA achieve comparable accuracy (best accuracy is 99.32% for CCA and 98.20% for DCA), and DCA appears to be much faster and computationally efficient than CCA, the DCA seems to be a good compromise between the processing time and the performance.

4) PERFORMANCE ANALYSIS AND VISUALIZATION

To further analyze the performance of the proposed method, we present the confusion matrix obtained by considering the results of fusing Fc. 7 and subset 3, and by SVM classifier (Table 12). This matrix shows to which variety test samples were classified, which allows having a deeper understanding on the method performance. Note that the top row represents the targeted classes, the leftmost column is for the predicted classes, where the rightmost column includes the proportion of the correctly classified samples to the total number of test samples in each date fruit variety. Noting also that varieties are numbered as follows 1) Ajina, 2) Ghars, 3) Hamraya, 4) Deglet, 5) Litima, 6) Loullou, 7) Tanslit, 8) Tantbucht, 9) Tarmount, 10) Techbeh Tati, 11)Tinisin, 12) Adam Deglet Nour, 13) Tivisyauin, 14) Bayd Hmam, 15) Bouaarus, 16) Degla bayda, 17) Deglet kahla, 18) Deglet ghabia, 19) Dfar lgat and 20) Dgoul.

From this confusion matrix, it evidently appears that most test samples were correctly classified. Nevertheless, some other samples were misclassified. For instance, two samples from Tanslit were misclassified to Tinisin variety, and one sample from Deglet ghabia was misclassified to Deglet kahla variety. This may be attributed to the huge visual resemblance between the samples from those varieties. For the sake of illustration, we present some date fruit samples from these varieties which are visually similar (FIGURE 14). Moreover, despite that mature dates from Tinisin are very similar,



**FIGURE 14.** Highly similar date samples from different varieties, from top to bottom and from left to right those varieties are Deglet kahla, Deglet, Tinisin, Tanslit, Deglet ghabia and Dgoul.

in terms of color and shape as well, to those from Dgoul, the proposed method has not confused them. Nonetheless, there are certain other confused varieties that do not resemble each other. For instance, despite that they do not look alike, one test sample from Hamraya were misclassified to Loullou variety.

5) COMPARISON WITH STATE OF THE ART

We compare the proposed method with several deep and handcrafted methods from the state of the art. In particular, we assess the performance of the methods in [7], [11], [12], [14], and [15]. These methods adopt hand-designed features along with conventional classifiers for date fruit classification. We also consider comparing our method with deep learning-based methods in [25] (VGG-16), [16] (MobileNet) and [17] (ResNet-50). For a fair comparison, we consider a fine tuning process of these deep networks. At first, data augmentation has been carried out by randomly altering rotation, width/height shift, zoom, brightness, and horizontal/vertical flip of newly generated samples. Regarded the process of the fine-tuning, the base-model of each network has been frozen. Then, a dense layer of 512 neurons jointly with a Soft-Max layer have been linked to the base-model and, later



TABLE 13. Comparison with state of the art methods.

Method	Description	Accuracy
[11]	RGB color features + Probabilistic Neural Network	30.03%
[12]	Morphological + color features + Gray-Level Co-occurrence Matrix + Artificial Neural Network	63.11%
[14]	Local Binary Patterns + Weber Local Descriptor + SVM	65.70%
[15]	Color histogram + GLCM + shape features + Gaussian Mixture Model	71.65%
[7]	Color histogram + Gray-Level Co-occurrence Matrix + shape features + outlier removal + Gaussian Mixture Model	74.24%
[25]	Fine-tuned VGG-16	88.58%
[17]	Fine-tuned ResNet-50	88.27%
[16]	Fine-tuned MobileNet	87.96%
<b>Our method</b>	VGG-F + PCANet + DCA	<b>98.20%</b>
	VGG-F + PCANet + CCA	<b>99.32%</b>

on, fine-tuned to fit our new dataset. Table 13 summarizes the compared works and the accuracies they obtained on our dataset.

From Table 13, on the one hand, by considering the DCA for networks fusion, it can be seen that the proposed method has significantly outperformed the methods of [7], [11], [12], [14], and [15] with 68.17%, 35.09%, 32.5%, 26.55% and 23.96%, respectively. In view of the challenges associated with our dataset (e.g., highly similar date varieties), the generalization capabilities of these methods have been dramatically influenced as they are hand-designed. The method in [7] has shown the best performance compared to the remaining handcrafted approaches as it considers pruning the dataset before performing the training process. In addition, this method adopts a multi-modal model that takes into account the intra-variability within each variety e.g., difference in maturity level. On the other hand, methods based on deep learning have shown better performance than the formerly cited ones. The proposed method outperforms the methods in [16], [17], and [25] by 9.62%, 9.93% and 10.24%, respectively. These results confirms once again the effectiveness of the proposed method.

## VI. CONCLUSION

In this paper, we proposed a method for date fruit type classification based on fusing supervised and unsupervised deep networks at feature-level. Discriminant correlation analysis (DCA) algorithm was used to combine features extracted using two kinds of networks namely VGG-F and PCANet. DCA has the advantage of simultaneously carrying out feature fusion and dimensionality reduction with a low com-

putational complexity. As a second contribution, we have introduced a new date fruit benchmark, which includes date fruit images from 20 date varieties. This benchmark is, to the best of our knowledge, the largest one in terms of number of varieties. It involves date samples with different flavor, shape, size, color, maturity level and hardness degree. Experimental results have demonstrated that DCA has successfully improved the individual decisions yielded by each of VGG-F and PCANet, which proved the complementarity of features learned from those networks. Furthermore, the proposed method has outperformed several state of the art methods. As a future work, one can investigate integrating handcrafted features to complement deep-based features. Another track is to adapt existing deep networks to construct a network specific to the task of date fruit sorting.

## REFERENCES

- [1] (2019). *Food and Agriculture Organization of the United Nations*. [Online]. Available: <https://www.fao.org/faostat/en/#data/QCL/visualize>
- [2] K. Hameed, D. Chai, and A. Rassau, "Class distribution-aware adaptive margins and cluster embedding for classification of fruit and vegetables at supermarket self-checkouts," *Neurocomputing*, vol. 461, pp. 292–309, Oct. 2021.
- [3] A. Nasiri, A. Taheri-Garavand, and Y.-D. Zhang, "Image-based deep learning automated sorting of date fruit," *Postharvest Biol. Technol.*, vol. 153, pp. 133–141, Jul. 2019.
- [4] S. Al-Rahbi, A. Manickavasagan, and G. Thomas, "Back propagation neural network (BPNN) to detect surface crack on dates using RGB images," *J. Med. Bioeng.*, vol. 4, no. 1, pp. 67–70, 2015.
- [5] B. D. Pérez-Pérez, J. P. García Vázquez, and R. Salomón-Torres, "Evaluation of convolutional neural networks' hyperparameters with transfer learning to determine sorting of ripe Medjool dates," *Agriculture*, vol. 11, no. 2, p. 115, Feb. 2021.
- [6] M. Faisal, F. Albogamy, H. Elgibreen, M. Algabri, and F. A. Alqershi, "Deep learning and computer vision for estimating date fruits type, maturity level, and weight," *IEEE Access*, vol. 8, pp. 206770–206782, 2020.
- [7] O. Aiadi, M. L. Kherfi, and B. Khaldi, "Automatic date fruit recognition using outlier detection techniques and Gaussian mixture models," *ELCVIA, Electron. Lett. Comput. Vis. Image Anal.*, vol. 18, no. 1, pp. 52–75, 2019.
- [8] W. S. Alhamdan and J. M. Howe, "Classification of date fruits in a controlled environment using convolutional neural networks," in *Proc. Int. Conf. Adv. Mach. Learn. Technol. Appl.* Cham, Switzerland: Springer, 2021, pp. 154–163.
- [9] J. Naranjo-Torres, M. Mora, R. Hernández-García, R. J. Barrientos, C. Fredes, and A. Valenzuela, "A review of convolutional neural network applied to fruit image processing," *Appl. Sci.*, vol. 10, no. 10, p. 3443, May 2020.
- [10] A. I. Hobani, A. M. Thottam, and K. A. M. Ahmed, "Development of a neural network classifier for date fruit varieties using some physical attributes," King Saud Univ.-Agric. Res. Center, Riyadh, Saudi Arabia, Tech. Rep., 2003, pp. 5–18, vol. 126.
- [11] M. Fadel, "Date fruits classification using probabilistic neural networks," *Agricult. Eng. Int., CIGR J.*, vol. 4, pp. 1–6, Dec. 2007.
- [12] A. Haidar, H. Dong, and N. Mavridis, "Image-based date fruit classification," in *Proc. 4th Int. Congr. Ultra Mod. Telecommun. Control Syst.*, Oct. 2012, pp. 357–363.
- [13] A. A. A. Sen, N. M. Bahbouh, A. B. Alkhodre, A. M. Aldhawi, F. A. Aldham, and M. I. Aljabri, "A classification algorithm for date fruits," in *Proc. 7th Int. Conf. Comput. Sustain. Global Develop. (INDIACom)*, Mar. 2020, pp. 235–239.
- [14] G. Muhammad, "Date fruits classification using texture descriptors and shape-size features," *Eng. Appl. Artif. Intell.*, vol. 37, pp. 361–367, Jan. 2015.
- [15] A. Oussama and M. L. Kherfi, "A new method for automatic date fruit classification," *Int. J. Comput. Vis. Robot.*, vol. 7, no. 6, pp. 692–711, 2017.

- [16] M. A. Khayer, M. S. Hasan, and A. Sattar, "Arabian date classification using CNN algorithm with various pre-trained models," in *Proc. 3rd Int. Conf. Intell. Commun. Technol. Virtual Mobile Netw. (ICICV)*, Feb. 2021, pp. 1431–1436.
- [17] A. Al-Sabaawi, "Employment of pre-trained deep learning models for date classification: A comparative study," in *Proc. Int. Conf. Intell. Syst. Design Appl.* Cham, Switzerland: Springer, 2020, pp. 181–189.
- [18] A. Magsi and J. A. S. H. M. Danwar, "Date fruit recognition using feature extraction techniques and deep convolutional neural network," *Indian J. Sci. Technol.*, vol. 12, no. 32, pp. 1–12, Aug. 2019.
- [19] M. S. Hossain, G. Muhammad, and S. U. Amin, "Improving consumer satisfaction in smart cities using edge computing and caching: A case study of date fruits classification," *Future Gener. Comput. Syst.*, vol. 88, pp. 333–341, Nov. 2018.
- [20] T. Najeeb and M. Safar, "Dates maturity status and classification using image processing," in *Proc. Int. Conf. Comput. Sci. Eng. (ICCSE)*, Mar. 2018, pp. 1–6.
- [21] A. Septiarini, H. Hamdani, H. R. Hatta, and A. A. Kasim, "Image-based processing for ripeness classification of oil palm fruit," in *Proc. 5th Int. Conf. Sci. Inf. Technol. (ICSITech)*, Oct. 2019, pp. 23–26.
- [22] R. Pourdarbani, H. R. Ghassemzadeh, H. Seyedarabi, F. Z. Nahandi, and M. M. Vahed, "Study on an automatic sorting system for date fruits," *J. Saudi Soc. Agricult. Sci.*, vol. 14, no. 1, pp. 83–90, 2015.
- [23] D. B. Pérez-Pérez, R. Salomón-Torres, and J. P. García-Vázquez, "Dataset for localization and classification of Medjool dates in digital images," *Data Brief*, vol. 36, Jun. 2021, Art. no. 107116.
- [24] M. Faisal, M. Alsulaiman, M. Arafah, and M. A. Mekhtiche, "IHDS: Intelligent harvesting decision system for date fruit based on maturity stage using deep learning and computer vision," *IEEE Access*, vol. 8, pp. 167985–167997, 2020.
- [25] H. Altaheri, M. Alsulaiman, and G. Muhammad, "Date fruit classification for robotic harvesting in a natural environment using deep learning," *IEEE Access*, vol. 7, pp. 117115–117133, 2019.
- [26] A. Hakami and M. Arif, "Automatic inspection of the external quality of the date fruit," *Proc. Comput. Sci.*, vol. 163, pp. 70–77, Jan. 2019.
- [27] A. Manickavasagan, N. K. Al-Mezeini, and H. N. Al-Shekailli, "RGB color imaging technique for grading of dates," *Scientia Horticulturae*, vol. 175, pp. 87–94, Aug. 2014.
- [28] Z. Guo, M. Zhang, D.-J. Lee, and T. Simons, "Smart camera for quality inspection and grading of food products," *Electronics*, vol. 9, no. 3, p. 505, Mar. 2020.
- [29] A. S. Alturki, "Date fruits grading and sorting classification algorithm using colors and shape features," *Int. J. Eng. Res. Technol.*, vol. 13, no. 8, pp. 1917–1920, 2020.
- [30] N. Alavi, "Quality determination of Mozafati dates using Mamdani fuzzy inference system," *J. Saudi Soc. Agricult. Sci.*, vol. 12, no. 2, pp. 137–142, Jun. 2013.
- [31] L. Hamrouni, M. L. Kherfi, O. Aiadi, and A. Benbelghit, "Plant leaves recognition based on a hierarchical one-class learning scheme with convolutional auto-encoder and Siamese neural network," *Symmetry*, vol. 13, no. 9, p. 1705, Sep. 2021.
- [32] B. Khaldi, O. Aiadi, and M. L. Kherfi, "Combining colour and grey-level co-occurrence matrix features: A comparative study," *IET Image Process.*, vol. 13, no. 9, pp. 1401–1410, Jul. 2019.
- [33] K. Simonyan and A. Zisserman, "Very deep convolutional networks for large-scale image recognition," 2014, *arXiv:1409.1556*.
- [34] K. Chatfield, K. Simonyan, A. Vedaldi, and A. Zisserman, "Return of the devil in the details: Delving deep into convolutional nets," 2014, *arXiv:1405.3531*.
- [35] T.-H. Chan, K. Jia, S. Gao, J. Lu, Z. Zeng, and Y. Ma, "PCANet: A simple deep learning baseline for image classification?" *IEEE Trans. Image Process.*, vol. 24, no. 12, pp. 5017–5032, Dec. 2015.
- [36] A. Korichi, S. Slatnia, and O. Aiadi, "TR-ICANet: A fast unsupervised deep-learning-based scheme for unconstrained ear recognition," *Arabian J. Sci. Eng.*, vol. 2022, pp. 1–12, Jan. 2022.
- [37] M. Haghghat, M. Abdel-Mottaleb, and W. Alhalabi, "Discriminant correlation analysis: Real-time feature level fusion for multimodal biometric recognition," *IEEE Trans. Inf. Forensics Security*, vol. 11, no. 9, pp. 1984–1996, Sep. 2016.
- [38] Q.-S. Sun, S.-G. Zeng, Y. Liu, P.-A. Heng, and D.-S. Xia, "A new method of feature fusion and its application in image recognition," *Pattern Recognit.*, vol. 38, no. 12, pp. 2437–2448, Dec. 2005.



**OUSSAMA AIADI** received the M.Sc. and Ph.D. degrees from Université Kasdi Merbah, Algeria, in 2013 and 2017, respectively. He is currently an Associate Professor with the Department of Computer Science and Information Technology, Université Kasdi Merbah. His current research interests include computer vision and machine learning.



**BELAL KHALDI** received the M.Sc. and Ph.D. degrees from Université Kasdi Merbah, Algeria, in 2012 and 2017, respectively. He is currently an Associate Professor with the Department of Computer Science and Information Technology, Université Kasdi Merbah. His current research interests include image processing and machine learning.



**MOHAMMED LAMINE KHERFI** received the B.S. degree in computer science from the National Institute of Computer Science, Algeria, and the M.Sc. and Ph.D. degrees in computer science from the Université de Sherbrooke, Canada. From 2005 to 2013, he was a Professor with the Department of Computer Science, Université du Québec à Trois-Rivières (UQTR), Canada. He is currently a Professor with the Department of Computer Science, University of Kasdi Merbah, Ouar

gla, Algeria, and the General Director of digitization and networks at the Ministry of Higher Education. He holds a U.S. patent. His research interests include image and multimedia processing, computer vision, and machine learning.



**MOHAMED LAMINE MEKHALFI** received the M.Sc. degree in electronics from the University of Hadj Lakhdar, Batna, Algeria, in 2012, and the Ph.D. degree in information and communication technology from the University of Trento, Italy, in 2016. He served for a year as a Postdoctoral Researcher with the Department of Pattern Analysis and Computer Vision (PAVIS), Italian Institute of Technology. Then he worked as a Researcher at Metacortex s.r.l., Trento. He joined Fondazione

Bruno Kessler (FBK) in 2021, as a Researcher at the Technologies of Vision Unit. His research interests include artificial intelligence and remote sensing.



**ABDULLAH ALHARBI** received the M.Sc. degree in information technology from the Rochester Institute of Technology, Rochester, NY, USA, and the master's degree in information assurance and cybersecurity and the Ph.D. degree in computer science from the Florida Institute of Technology, Melbourne, FL, USA, where he also got Information Assurance and Cybersecurity Graduate Certificate. He is currently an Assistant Professor of computer science at King Saud University, Riyadh,

Saudi Arabia. He is also the Dean of the College of Applied Computer Sciences, King Saud University, Muzahimiyah Branch. He is also the CEO of the Information Security Association, Hemaya, a non-profit organization, Saudi Arabia. He is also a Research Fellow at the Center of Excellence for Information Assurance, King Saud University. He was previously Department of Administrative Sciences Chair at the Community College, King Saud University. His research interests include wearable devices security, transparent and continuous security, alternative authentication, usable security, and behavioral biometrics.

• • •